

The chemical bonding and electronic structure of RhC, RhN, and RhO by anion photoelectron spectroscopy

Xi Li and Lai-Sheng Wang^{a)}

Department of Physics, Washington State University, 2710 University Drive, Richland, Washington 99352-1671 and W. R. Wiley Environmental Molecular Sciences Laboratory, Pacific Northwest National Laboratory, MS K8-88, P.O. Box 999, Richland, Washington 99352

(Received 2 June 1998; accepted 23 June 1998)

The electronic structure and chemical bonding of RhC, RhN, and RhO were experimentally investigated using anion photoelectron spectroscopy. Vibrationally resolved photoelectron spectra of RhC^- , RhN^- , and RhO^- were obtained at two detachment photon energies, 532 (2.33 eV) and 355 nm (3.49 eV). Electron affinities, low-lying electronic states, and vibrational frequencies are reported for the neutral diatomic molecules. The adiabatic electron affinities are similar for the three molecules and increase slightly from RhC to RhO (RhC: 1.46; RhN: 1.51; RhO: 1.58 eV). The low-lying electronic states are rather simple for RhC, with its first electronic excited state occurring at 9400 cm^{-1} above the ground state, whereas those of RhN and RhO are more complicated, with numerous closely spaced low-lying electronic states. Excited states of the anions were also observed for RhC^- and RhN^- . The trend of the chemical bonding from RhC to RhO is discussed based on the experimental results. © 1998 American Institute of Physics. [S0021-9606(98)00337-7]

I. INTRODUCTION

Rhodium; and its oxides and complexes, is a widely used transition metal catalyst from hydrocarbon conversions to nitrogen fixation.¹ Thus, understanding the chemical bonding between Rh and C, N, and O is of both basic and applied interest. The simple Rh diatomic molecules, RhC, RhN, and RhO, serve as prototypes for this purpose. However, little experimental information is known about these molecules.² Among the three diatomic molecules, RhC has been studied more extensively.²⁻⁴ The ground state and several low-lying excited states are known for RhC. On the other hand, there has been little experimental work on RhO.² To our best knowledge, RhN has never been studied experimentally prior to this work. Nevertheless, theoretical studies have been performed on RhN and RhO. Shim *et al.* recently carried out a detailed theoretical investigation of the electronic structure and bonding in RhN.⁵ RhO has been briefly studied in two previous theoretical investigations of Rh compounds.^{6,7}

In this paper, we report an experimental study of the electronic structure of RhC, RhN, and RhO using anion photoelectron spectroscopy (PES). Electron affinities (EAs), low-lying electronic states, and vibrational information are obtained for all three molecules. The observed electronic states are compared to and interpreted with available theoretical results.

II. EXPERIMENT

The experimental apparatus used for this study has been described in detail before.^{8,9} Briefly, it consists of a magnetic-bottle time-of-flight (TOF) photoelectron analyzer, a laser vaporization cluster source, and a TOF mass spec-

rometer. To generate the desired anionic species, a pure Rh disk target was laser-vaporized with a helium carrier gas seeded with CH_4 (5%), N_2 (5%), and O_2 (0.5%) for producing RhC^- , RhN^- , and RhO^- , respectively. The anions produced in the source were mass analyzed by the TOF mass spectrometer. The diatomic species of interest were mass selected and decelerated before being intercepted by the output of a Nd:YAG laser. Two detachment photon energies were used for the current set of experiments: 532 (2.33 eV) and 355 nm (3.49 eV). The obtained PES spectra are shown collectively in Fig. 1 for RhC^- , RhN^- , and RhO^- . The energy resolution was about 30 meV for 1 eV electrons, as calibrated using the spectrum of Rh^- .^{10,11}

III. RESULTS AND DISCUSSION

The chemical bonding between Rh and C (or N and O) mainly involves the $4d$ and $5s$ valence orbitals of Rh and the $2p$ orbitals of C (or N and O). Figure 2 illustrates schematically the valence molecular orbitals (MOs) derived from these valence atomic orbitals.³⁻⁵ The 11σ and 5π are bonding MOs between the $4d$ and $2p$ orbitals, whereas the 13σ and 6π can be viewed as the antibonding MOs between $4d$ and $2p$. The 12σ is a nonbonding MO of mainly $5s$ character. The occupancies of the 11σ , 5π , and 2δ MOs are the same for all three molecules. The differences between them result from the different occupations of the 12σ and 6π orbitals. The Rh–C bonding is characterized as a triple bond with a very high dissociation energy ($D_0=5.97\text{ eV}$),³ whereas the Rh–O bond is weaker ($D_0=4.2\text{ eV}$)² due to the occupation of the antibonding MOs. The ground state symmetry and MO configurations are known to be $X^2\Sigma^+(\cdots 12\sigma^1 6\pi^0)$, $X^1\Sigma^+(\cdots 12\sigma^2 6\pi^0)$, and $X^4\Sigma^-(\cdots 6\pi^2 12\sigma^1)$ for RhC,^{3,4} RhN,⁵ and RhO,^{6,7} respectively. With this basic electronic structure information, we

^{a)} Author to whom correspondence should be addressed.

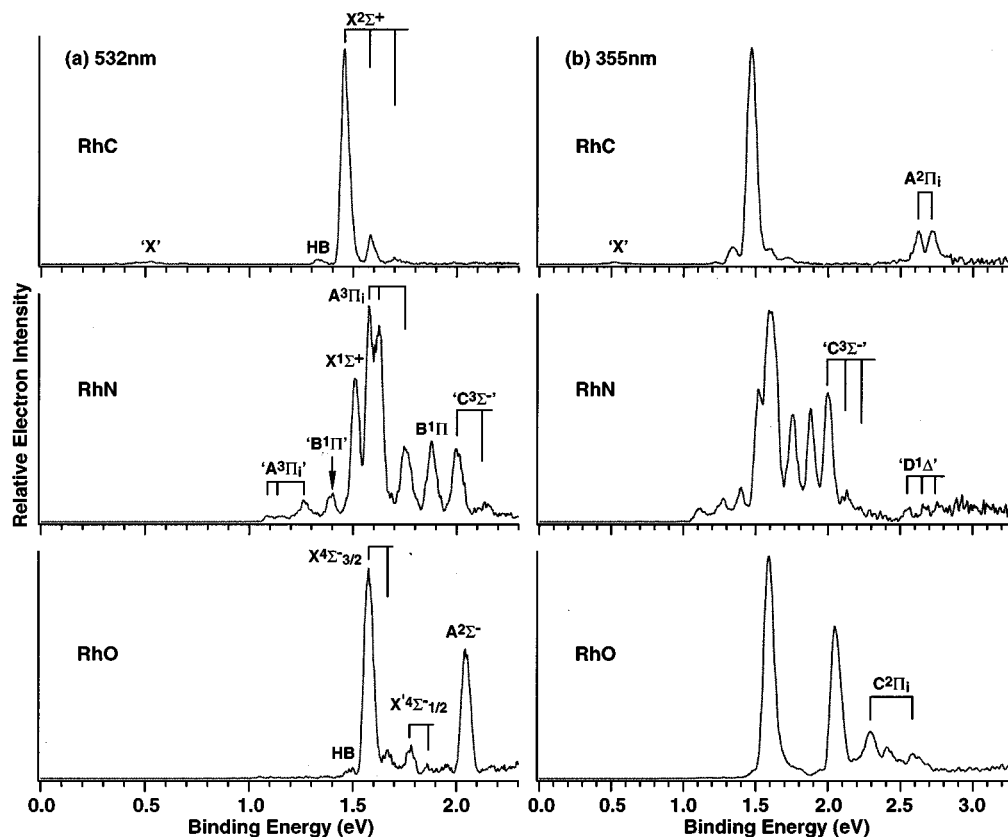


FIG. 1. Photoelectron spectra of RhC^- , RhN^- , and RhO^- at (a) 532 (2.33 eV) and (b) 355 nm (3.49 eV). HB stands for hot band transitions. Transitions due to excited states of the anions are labeled with single quotes. Vertical lines represent vibrational levels or spin-orbit components. See text for the assignments.

interpret and discuss the PES spectra and energy levels of the three molecules individually in the following.

A. RhC^- and RhC^-

The 532 nm spectrum of RhC^- shows a well-resolved vibrational progression starting at 1.46 eV with a vibrational spacing of about 1000 cm^{-1} . The intense peak represents the ground state of RhC and yields an adiabatic EA of 1.46 eV for RhC . A weak hot band was observed, giving a vibrational frequency for the RhC^- ground state also of about 1000 cm^{-1} . A very weak signal was observed in some spectra at about 0.53 eV, labeled as 'X,' which was most likely due to an electronically excited state of RhC^- . The 355 nm spectrum of RhC^- reveals two more transitions at 2.62 and 2.72 eV due to two excited states of RhC .

As mentioned above, RhC has been studied most extensively among the three molecules concerned in the current investigation. Its ground state and several low-lying excited states are known,²⁻⁴ making the interpretation and assignment of the PES spectra of RhC^- rather straightforward. The first excited state of RhC is a ${}^2\Pi$ state involving a transition from the 12σ to 6π orbital. Excitation energies of the two spin-orbit components (${}^2\Pi_{3/2,1/2}$) known previously are in excellent agreement with those of the two excited state features observed in the 355 nm spectrum of RhC^- , as shown in Table I.

In RhC^- , the extra electron can enter either the 6π orbital with a ground state configuration of $\cdots 12\sigma^1 6\pi^1 (X^3\Pi)$

or the 12σ orbital with a ground state of $X^1\Sigma^+(\cdots 12\sigma^2 6\pi^0)$. From the latter configuration it would require a two-electron transition to reach the ${}^2\Pi$ excited state. Although such multielectron transitions have been observed in anion PES of $3d$ oxide diatomics,^{12,13} they are expected to have low cross sections. Therefore, $12\sigma^1 6\pi^1$ is a more reasonable configuration for the ground state of RhC^- . Detachment of the single 6π electron of RhC^- then results in the $X^2\Sigma^+$ ground state of RhC , and removal of the single 12σ electron leads to the ${}^2\Pi_{3/2,1/2}$ excited state. The intensity ratio of the two spin-orbit components should be 2:1. The observation that their intensities appeared to be equal was probably due to a contribution from the $v=1$ level

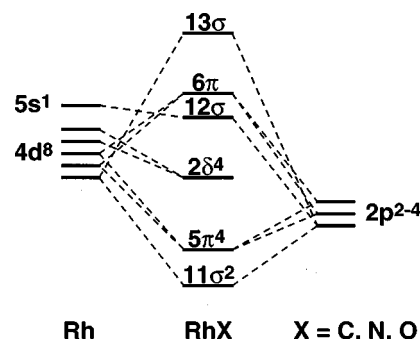


FIG. 2. Schematic diagram showing the correlation of the valence molecular orbitals of RhX with the valence atomic orbitals of Rh and X ($\text{X}=\text{C}, \text{N}, \text{O}$). The 11σ , 5π , and 2δ molecular orbitals are fully occupied in all three molecules, which have different occupancies in the 12σ and 6π orbitals.

TABLE I. Observed binding energies (BE) and measured spectroscopic constants for RhC⁻ and RhC.

	BE (eV)	Term value (cm ⁻¹)		Vib. freq. (cm ⁻¹)	
		Current	Previous ^a	Current	Previous ^a
RhC ⁻	$X^3\Pi(12\sigma^16\pi^1)$	0	0	1000(60)	
	$A^1\Sigma^+(12\sigma^26\pi^0)$	0.53(5)	7500(200)		
RhC	$X^2\Sigma^+(12\sigma^16\pi^0)$	1.46(2) ^b	0	1000(60)	1049.87
	$A^2\Pi_{3/2}(12\sigma^06\pi^1)$	2.62(3)	9400(100)	9462.94	949.41
	$^2\Pi_{1/2}$	2.72(3)	10 200(100)		939.12
			10 242.75		

^aFrom Reference 2.^bAdiabatic electron affinity of RhC.

of $^2\Pi_{3/2}$ to that of the $^2\Pi_{1/2}$ peak because the vibrational frequency and the spin-orbit splitting are very similar (Table I).

We assign the very weak signal at 0.53 eV to be from an excited state of RhC⁻, resulting from the configuration $12\sigma^26\pi^0(^1\Sigma^+)$. This excited state is metastable as the relaxation to the anion ground state is spin-forbidden. We have observed such metastable anionic excited states in several transition metal oxide systems previously.^{14,15} The observed binding energies and the obtained spectroscopic information for RhC and RhC⁻ are listed in Table I.

B. RhN and RhN⁻

The PES spectra of RhN⁻ (Fig. 1) are much more complicated than those of RhC⁻. Eleven detachment features were observed in the 532 nm spectrum between 1 and 2.2 eV binding energies, and more features with weak intensity were further revealed beyond 2.5 eV in the 355 nm spectrum. None of the features can be assigned to vibrational progressions, except for the 2.00 and 2.12 eV features, which were identified as a vibrational progression, as shown in both the 532 and 355 nm spectra. The binding energies of the observed features are given in Fig. 3 with the assigned transitions, as discussed next.

From the MO picture shown in Fig. 2 and the discussion above for RhC⁻, it is expected that the ground state MO configuration of RhN can be either $\cdots 12\sigma^26\pi^0(X^1\Sigma^+)$ or $\cdots 12\sigma^16\pi^1(X^3\Pi)$. Shim *et al.* recently performed a detailed theoretical study on RhN.⁵ They calculated the ground and several excited states with relativistic corrections. The predicted ground state of RhN is $X^1\Sigma^+$ with two low-lying excited states, $A^3\Pi$ and $B^1\Pi$, both derived from the $\cdots 12\sigma^16\pi^1$ configuration. The $A^3\Pi$ state was predicted to be about 1825 cm⁻¹ above the ground state with four closely spaced spin-orbit states; the $B^1\Pi$ state was predicted to be 3360 cm⁻¹ above the ground state.

In the ground state of RhN⁻, the extra electron should occupy the 6π MO, and the following one-electron detachment channels are expected, leading to the ground and low-lying excited states of RhN,

$$\cdots 12\sigma^26\pi^1(^2\Pi) \rightarrow \cdots 12\sigma^26\pi^0, X^1\Sigma^+ \quad (1)$$

$$\rightarrow \cdots 12\sigma^16\pi^1, A^3\Pi_{0,1,2}, B^1\Pi. \quad (2)$$

Even with the spin-orbit components, the observed PES features are more numerous than the above derived transitions. We noted that the first four weak features between 1.1 and 1.4 eV show exactly the same spacing as those four intense features at higher binding energies between about 1.6 and 1.9 eV (Fig. 1), implying that they represent the same set of neutral electronic states. This observation is important, suggesting that the first four weak features should be due to transitions from an excited state of RhN⁻, consistent with the fact that their relative intensities were observed to vary slightly at different experimental conditions.

Therefore, we assign the strong peak at 1.51 eV as the transition from the ground state of the anion to the ground state of RhN ($X^1\Sigma^+$), yielding an adiabatic EA of 1.51 eV for RhN. The next three intense features at 1.58, 1.63, and 1.75 eV are assigned to the spin-orbit components of the $A^3\Pi_i$ state. The peak at 1.88 eV is assigned to the $B^1\Pi$ state. Thus, we see that the $A^3\Pi$ state is nearly degenerate to the ground state. The $^3\Pi_0$ component is only 0.07 eV above the ground state, which was barely resolved in the 355 nm spectrum. The calculated spin-orbit levels for the $^3\Pi$ state are consistent with, but do not agree quantitatively with our experimental measurements. However, the calculated ex-

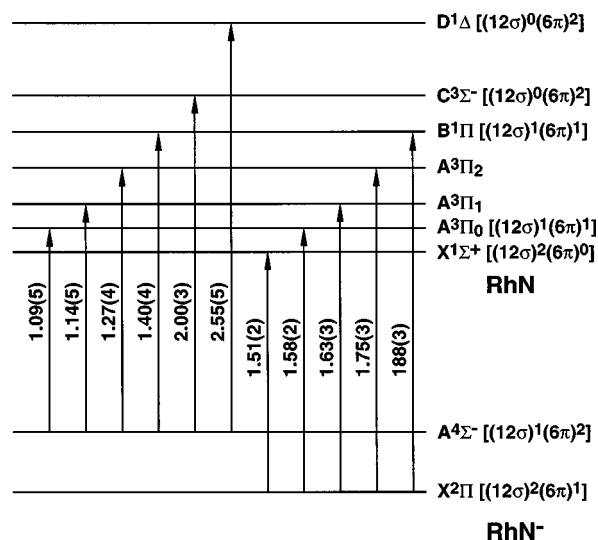


FIG. 3. Schematic energy levels showing the measured binding energies (eV) of detachment transitions from the ground and excited states of RhN⁻ to those of RhN.

TABLE II. Measured electronic energy levels (cm^{-1}) for RhN^- and RhN compared to previous calculations.^a

		Current measurement (cm^{-1})	Previous calculation (cm^{-1}) ^a
RhN^-	$X \ ^2\Pi(12\sigma^26\pi^1)$	0	
	$A \ ^4\Sigma^-(12\sigma^16\pi^2)$	3900(100)	
RhN	$X \ ^1\Sigma^+(12\sigma^26\pi^0)$	0	0
	$A \ ^3\Pi_0(12\sigma^16\pi^1)$	560(50)	1825($\Omega=0^+$), 1972($\Omega=0^-$)
	$\ ^3\Pi_1$	970(90)	2112($\Omega=2$)
	$\ ^3\Pi_2$	1900(100)	3074($\Omega=1$) ^b
	$B \ ^1\Pi(12\sigma^16\pi^1)$	3000(100)	3360($\Omega=1$) ^b
	$C \ ^3\Sigma^-(12\sigma^06\pi^2)$	7800(100)	8223
	$D \ ^1\Delta(12\sigma^06\pi^12)$	12 300(200)	14 062

^aFrom Reference 5.^bThe calculation indicates that these spin-orbit coupled states have equal contributions from the $^3\Pi$ and $^1\Pi$ non-spin-orbit coupled states.

citation energy for the $B \ ^1\Pi$ level is in excellent agreement with our measurement as shown in Table II.

The near degeneracy between the $\cdots 12\sigma^26\pi^0$ and $\cdots 12\sigma^16\pi^1$ configurations for RhN suggests that the $^4\Sigma^-(\cdots 12\sigma^16\pi^2)$ state would be a likely candidate for the excited state of RhN^- . This excited state of the anion can lead to the following one-electron detachment channels:

$$\cdots 12\sigma^16\pi^2(^4\Sigma^-) \rightarrow \cdots 12\sigma^16\pi^1, \ ^3\Pi_{0,1,2}, \ ^1\Pi \quad (3)$$

$$\rightarrow \cdots 12\sigma^06\pi^2, \ ^3\Sigma^-, \ ^1\Delta, \ ^1\Sigma^- \quad (4)$$

Note that from this anionic excited state one cannot reach the ground state of the neutral through a one-electron detachment. Further note that the detachment channel (3) results in the same set of states as that of detachment channel (2) from the anionic ground state. Therefore, the four weak features at low binding energies are naturally due to the transitions described in (3). These are shown in Fig. 1, where detachment features from excited anionic states are labeled with single quotes. It was noted that the relative intensities of the features due to detachment from the excited anionic state seemed to be different from those due to detachment of the ground state RhN^- . In particular, the intensities of the 'A $^3\Pi_2$ ' and 'B $^1\Pi$ ' peaks appeared to be high, which was probably due to contributions from hot band transitions associated with the $X \ ^1\Sigma^+$ and $A \ ^3\Pi_i$ features.

The second one-electron detachment channel (4) from the anionic excited state can result in three more RhN excited states, which cannot be reached from the ground state of the anion through one-electron detachment. Among the three states given in (4) above, the $^3\Sigma^-$ and $^1\Delta$ states were calculated by Shim *et al.* with predicted excitation energies at 8223 and 14 062 cm^{-1} , respectively. We assign the features at 2.0 and 2.5 eV to these two states, respectively. The measured excitation energies are in good agreement with the theoretical predictions. Both of these states were predicted to have longer bond lengths than that of the ground state, consistent with our observation of the vibrational progressions for these two states. The estimated vibrational frequency of 900(100) cm^{-1} for these two states is also consistent with those predicted, 817 and 831 cm^{-1} for the $^3\Sigma^-$ and $^1\Delta$ states, respectively. The features at high binding energies are weak and it is possible that there may be transitions due to

the unknown $^1\Sigma^-$ state, which was not calculated by Shim *et al.* The binding energies of all the detachment transitions between RhN^- and RhN are given in Fig. 3. The measured excitation energies of the low-lying states are summarized and compared to the theoretical predictions in Table II.

C. RhO and RhO^-

The 532 nm spectrum of RhO^- shows two strong peaks at 1.58 and 2.05 eV. The 1.58 eV peak should be due to the transition from the ground state of the anion to that of the neutral, and defines the adiabatic EA of RhO . A hot band and a vibrationally excited level were also observed around the 1.58 eV ground state peak, yielding a similar vibrational frequency of about 730 cm^{-1} for the ground states of both RhO^- and RhO . A weak feature at 1.78 eV was also observed in the 532 nm spectrum with a weak vibrational progression similar to that of the ground state. More features were revealed between 2.3 and 2.6 eV in the 355 nm spectrum, where the weak 1.78 eV feature was not well resolved.

Surprisingly, RhO has not been studied in detail theoretically, although it was investigated briefly in two previous theoretical studies about Rh compounds.^{6,7} The ground state of RhO was predicted to be $X \ ^4\Sigma^-(\cdots 6\pi^212\sigma^1)$ in the theoretical studies. The PES spectra of RhO^- can be interpreted straightforwardly with the following one-electron transitions by assuming that the extra electron enters the 12σ orbital:

$$\cdots 6\pi^212\sigma^2(^3\Sigma^-) \rightarrow \cdots 6\pi^212\sigma^1, \ X \ ^4\Sigma^-, \ A \ ^2\Sigma^- \quad (5)$$

$$\rightarrow \cdots 6\pi^112\sigma^2, \ C \ ^2\Pi_{3/2,1/2} \quad (6)$$

We assign the 1.58 and 2.05 eV peaks to the ground state ($X \ ^4\Sigma^-$) and the first excited state ($A \ ^2\Sigma^-$) of RhO , due to detachment of a spin-down and spin-up 12σ electron, respectively, through one-electron transitions. The high binding energy features are assigned to be due to the two spin-orbit states of $C \ ^2\Pi_{3/2,1/2}$, resulting from detachment channel (6). A vibrational progression was clearly seen for the $^2\Pi_{3/2}$ state with a frequency of about 800 cm^{-1} . The weak feature at 1.78 eV, which was not resolved clearly in the 355 nm spectrum, is tentatively assigned to the $\Omega=1/2$ component of the $X \ ^4\Sigma^-$ ground state. No low binding energy features due to anionic excited states were observed in the spectra of RhO^- compared to those of RhC^- and RhN^- . However, a close

TABLE III. Observed binding energies (BE) and measured spectroscopic constants for RhO^- and RhO .

		BE (eV)	Term value (cm^{-1})	Vib. freq. (cm^{-1})
RhO^-	$X^3\Sigma^-(6\pi^2 12\sigma^2)$		0	730(80)
RhO	$X^4\Sigma_{3/2}^-(6\pi^2 12\sigma^1)$	1.58(2) ^a	0	730(80)
	$^4\Sigma_{1/2}^-$	1.78(3)	1600(100)	730(80)
	$A^3\Sigma^-(6\pi^2 12\sigma^1)$	2.05(3)	3800(100)	
	$B^2\Pi_{3/2}(6\pi^1 12\sigma^2)$	2.29(3)	5700(100)	800(90)
	$^2\Pi_{1/2}$	2.59(3)	8100(100)	

^aAdiabatic electron affinity of RhO .

examination of the low binding energy side of the 532 nm spectrum of RhO^- did reveal very weak signals (<1% relative to the strongest feature), which were probably due to anionic excited states but could not be definitively identified because of their feeble intensities. Our observed binding energies and spectroscopic constants for RhO and RhO^- are given in Table III.

D. Trend of chemical bonding from RhC to RhO

The systematic study of the three diatomics of Rh offers an opportunity to probe the trend of chemical bonding from the carbide to the oxide. The electron affinities that we determined for the three molecules are very similar and increase slightly from RhC (1.46) to RhN (1.51) to RhO (1.58 eV). No substantial vibrational excitations were observed in any detachment transition of the three molecules, consistent with the nonbonding or slightly antibonding nature of the 12σ and 6π MOs (Fig. 2), from which all the detachment transitions occur. We observe that the ordering of the 12σ and 6π MOs undergo a gradual change from RhC to RhO . The separation between these two MOs is more than 1 eV in RhC , whereas they become nearly degenerate in RhN . In RhO , the 6π MO is actually slightly lower in energy than the 12σ . Although we could not directly probe the bonding MOs (i.e., 11σ and 5π), the gradual stabilization of the 6π antibonding MO from RhC to RhO indicates that the 5π bonding MO is gradually weakening from RhC to RhO , consistent with the known dissociation energies of RhC (5.97)³ and RhO (4.2 eV).² The dissociation energy of RhN has not been experimentally determined. The recent calculation by Shim *et al.* predicted a dissociation energy of 1.74 eV for RhN .⁵ This value is low, considering the trend from RhC to RhO . One would expect the dissociation energy of RhN to be between those of RhC and RhO . It is also interesting to note that while the first excited state of RhC is more than 1 eV above the ground state, both RhN and RhO have much more complicated and closely spaced low-lying energy levels. The complicated nature of the low-lying energy levels of both RhN and RhO is probably responsible for the fact that while the optical spectroscopy of RhC was measured long ago,² to date there has been no report of any optical experiments on

RhN and RhO . Thus, PES provides a relatively convenient, albeit less accurate, means to unravel the complicated spectroscopy of these seemingly simple diatomics.

IV. CONCLUSIONS

We report a systematic photoelectron spectroscopic study of RhC^- , RhN^- , and RhO^- at 532 and 355 nm detachment wavelengths. The experiments provide direct measurements of the electron affinities and low-lying electronic states of the neutral diatomics, as well as anionic excited state information in the cases of RhC^- and RhN^- . The spectra of RhC^- are simple and the obtained energies of the excited states agree with previous optical measurements. The spectra of RhN^- and RhO^- reveal that the low-lying electronic states of RhN and RhO are more complicated due to the near degeneracy of the 12σ and 6π outermost occupied MOs. The spectra of RhN^- provide a rigorous test for the recent theoretical calculations and indicate that the calculations including relativistic corrections describe the low-lying electronic states of RhN quite well.⁵ No detailed theoretical calculations are yet available for RhO . The current results provide spectroscopic information for both the anions and the neutrals of these simple Rh diatomic molecules and will be valuable to compare to future theoretical efforts and optical experiments.

ACKNOWLEDGMENTS

Support of this research by the National Science Foundation is gratefully acknowledged. The work was performed at Pacific Northwest National Laboratory, operated for the U.S. Department of Energy by Battelle, under Contract No. DE-AC06-76RLO 1830. L.S.W. is an Alfred P. Sloan Research Fellow.

- ¹ *Homogeneous Transition Metal Catalyzed Reactions*, edited by W. R. Moser and D. W. Slocum (American Chemical Society, Washington, DC 1992).
- ² K. P. Huber and G. Herzberg, *Molecular Spectra and Molecular Structure IV: Constants of Diatomic Molecules* (Van Nostrand Reinhold, New York, 1979).
- ³ I. Shim and K. A. Gingerich, *J. Chem. Phys.* **81**, 5937 (1984).
- ⁴ H. Tan, M. Liao, and K. Balasubramanian, *Chem. Phys. Lett.* **280**, 423 (1997).
- ⁵ I. Shim, K. Mandix, and K. A. Gingerich, *J. Mol. Struct.: THEOCHEM* **393**, 127 (1997).
- ⁶ G. J. Mains and J. M. White, *J. Phys. Chem.* **95**, 112 (1991).
- ⁷ P. E. M. Siegbahn, *Chem. Phys. Lett.* **201**, 15 (1993).
- ⁸ L. S. Wang, H. S. Cheng, and J. Fan, *J. Chem. Phys.* **102**, 9480 (1995).
- ⁹ L. S. Wang and H. Wu, in *Advances in Metal and Semiconductor Clusters*, edited by M. A. Duncan (JAI, Greenwich, 1998), Vol. 4, pp. 299–343.
- ¹⁰ C. S. Feigerle, R. R. Corderman, S. V. Bobashev, and W. C. Lineberger, *J. Chem. Phys.* **74**, 1580 (1981).
- ¹¹ C. E. Moore, *Atomic Energy Levels*, Natl. Bur. Stand. Circ. (U.S. GPO, Washington D.C. 1971), Vol. III.
- ¹² H. Wu and L. S. Wang, *J. Chem. Phys.* **107**, 8221 (1997).
- ¹³ Two-electron transitions have also been observed in the photoelectron spectra of ScO^- and YO^- , H. Wu and L. S. Wang, *J. Phys. Chem.* (submitted).
- ¹⁴ H. Wu, S. R. Desai, and L. S. Wang, *J. Phys. Chem. A* **101**, 2103 (1997).
- ¹⁵ H. Wu and L. S. Wang, *J. Chem. Phys.* **108**, 5310 (1998).